

## Identification of Amino Acid Residues Associated with Modulation of Flavin-Containing Monooxygenase (FMO) Activity by Imipramine: Structure/Function Studies with FMO1 from Pig and Rabbit

M. Keith Wyatt,<sup>‡,§</sup> Lila H. Overby,<sup>‡</sup> Michael P. Lawton,<sup>‡,||</sup> and Richard M. Philpot<sup>\*,‡</sup>

*Molecular Pharmacology Section, Laboratory of Signal Transduction, National Institute of Environmental Health Sciences, Research Triangle Park, North Carolina 27709, and Department of Toxicology, North Carolina State University, Raleigh, North Carolina 27695*

*Received October 22, 1997; Revised Manuscript Received February 24, 1998*

**ABSTRACT:** The activity of the flavin-containing monooxygenase (FMO) can be modulated by a number of nitrogen-containing compounds in a manner that is both isoform and modulator-dependent. We now show that the direction (activation or inhibition) and extent of modulation can also be dependent on substrate concentration. Imipramine activates methimazole metabolism catalyzed by rabbit FMO1 or FMO2 at methimazole concentrations greater than 50 or 100  $\mu$ M, respectively, and inhibits at lower methimazole concentrations. The extent of the activation increases as the substrate concentration increases, and the extent of inhibition increases as the substrate concentration decreases. With either inhibition or activation, the magnitude of the effect shows a similar, direct dependency on imipramine concentration. In contrast, imipramine inhibits the metabolism of methimazole catalyzed by pig FMO1 at all substrate concentrations. The structural basis for this unique ortholog difference between the responses of rabbit and pig FMO1 to imipramine was studied by random chimeragenesis and site-directed mutagenesis. Results with chimeras indicated that modulation of FMO1 activity by imipramine is controlled to a great extent by two areas of the FMO primary structure (residues 381–432 and 433–465). Four amino acids in these regions (positions 381, 400, 420 and 433) and one additional residue (position 186) were identified by site-directed mutagenesis as primary determinants of the imipramine response. When the residues at these positions in rabbit FMO1 are exchanged for the corresponding residues of pig FMO1, a mutant with the functional properties of pig FMO1 is produced. Our results suggest that the response of FMO1 to imipramine involves a distribution between two sites that is regulated by structural features that do not alter the overall binding. The inhibition observed, although it appears to be competitive, likely does not involve competition for a binding site since alteration of imipramine metabolism has no effect on the parameters of methimazole metabolism.

The mammalian microsomal flavin-containing monooxygenases (FMO) are xenobiotic metabolizing enzymes that catalyze the oxidation of nucleophilic nitrogen, sulfur, phosphorus, and selenium atomic centers present in a number of drugs, pesticides, and other environmental chemicals (1, 2). The FMO gene family consists of five members (FMO1–5) that exhibit 82–88% and 51–58% structural identity among orthologs and homologues, respectively (3). The presence of more than one form of FMO was suggested initially by the observation that  $Mg^{2+}$  and  $Hg^{2+}$  decrease hepatic FMO activity but increase the activity in lung (4). The existence of two forms of FMO, one in liver (FMO1) and one in lung (FMO2), was confirmed by determination of immunochemical and catalytic differences (5, 6). Subsequently, FMO1, cloned from pig (7) and rabbit liver (8), and FMO2, cloned from rabbit lung (8), were shown to be products of distinct genes. Three additional FMO isoforms

(FMO3, FMO4, and FMO5) have now been cloned and characterized (2, 3, 9).

One of the more interesting properties of the FMOs is isoform-dependent activation of catalytic activity by certain amines. Two distinct types of activation have been described, modulator induced and substrate induced (self-activation). For example, Ziegler et al. (10) showed that a number of short-chain primary amines, including *n*-octylamine, can enhance the oxidation of dimethylaniline catalyzed by pig FMO1, an isoform for which these amines are not substrates. Self-activation in the metabolism of some substrates (*N,N*-dimethyloctylamine and other *N,N*-dimethylalkylamines) but not others (dimethylaniline) was also observed (10). With FMO2, the results are quite different. First, *n*-octylamine is a substrate for FMO2 (11, 12) and is not an activator (13). Second, tricyclic antidepressants appear to enhance activity catalyzed by FMO2 but not FMO1 (13) and to be substrates for FMO1 and not FMO2 (14). These results and others (1) support the conclusion reached by Ziegler et al. (10) that the FMO contains distinct catalytic and regulatory sites.

\* To whom correspondence should be addressed.

<sup>‡</sup> National Institute of Environmental Health Sciences.

<sup>§</sup> North Carolina State University.

<sup>||</sup> Present Address: Central Research Division, Pfizer, Inc., Groton, CN 066340.

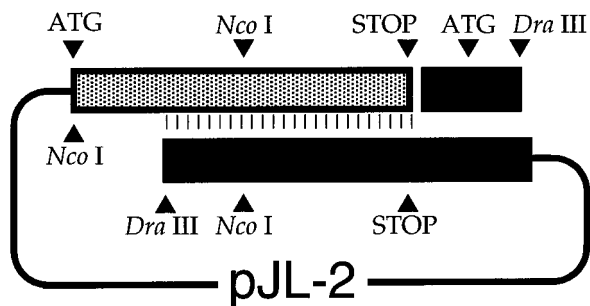


FIGURE 1: Diagram of the construct used for random chimeragenesis. The cDNA (start to stop) for rabbit FMO1 (spotted portion) was inserted in tandem with the cDNA (5' and 3' noncoding regions included) for pig FMO1 (solid portion) into the pJL-2 vector. The diagram depicts hybridization (|||) of the rabbit and pig FMO1 sequences hypothesized to take place with DNA that is cut once at the *Dra*III site unique to the pig FMO1 sequence. The *Nco*I sites were used to analyze for the formation of chimeras.

We have started to examine the molecular basis for the modulation of FMO-catalyzed activity by the tricyclic antidepressant, imipramine. The technique of random chimeragenesis (15, 16) has been used to exploit a major difference discovered between the responses of pig and rabbit FMO1 (87% identity) to imipramine. Results of these experiments and of site-directed mutagenesis show that the distinct responses of the FMO1 orthologs to imipramine are associated with as few as five of the 70 amino acid differences between the two forms of the enzyme. In addition to confirming the existence of distinct catalytic and regulatory sites on FMO1, our results are most easily explained by the presence of a second "catalytic" site associated with the metabolism of the modulator compound.

## MATERIALS AND METHODS

**FMO cDNAs and Expression Constructs.** The cDNA (coding region) encoding rabbit FMO1 (8) was cloned into the pJL-2 expression vector (17) as described previously (18). The cDNA (coding region) encoding rabbit FMO2 (8) was cloned into the pKKHC expression vector (19). Full-length cDNA encoding pig FMO1 (7) was contained in pBlueScript (pBS, Stratagene).

**Random Chimeragenesis.** The pJL-2-rabbit/pig FMO1 tandem construct (pJL-rb/pig FMO1) used for random chimeragenesis is shown in Figure 1. The development of this construct and its application to random chimeragenesis were based on the work of Chen et al. (15) and Kim and Devreotes (16). Full-length cDNA encoding pig FMO1 (2084 bp) was recovered from pBS by digestion with *Hinc*II and *Sma*I (New England Biolabs, Beverly, MA) and blunt-end ligated into an *Eco*RV site located 3' of the rabbit FMO1 stop codon in the pJL-2 rabbit FMO1 construct. The pJL-rb/pig FMO1 construct formed contained rabbit FMO1 and pig FMO1 in tandem with the 3'-end of rabbit FMO1 adjacent to the 5'-end of pig FMO1. cDNA (1  $\mu$ g, ~5 mL) encoding pJL-rb/pig FMO1 was obtained by alkaline lysis miniprep (20), linearized by digestion with *Dra*III and treated with 3 units of calf intestine alkaline phosphatase. (A unique *Dra*III site is located in the construct at the second base of codon 130 in the pig FMO1 sequence.) Linearized plasmid, purified on a Wizard DNA column (Promega, Madison, WI), was used to transform (heat-shock) RecA<sup>+</sup> strains of *Escherichia coli*, NM522 or JM101 (Stratagene), according

to the manufacturer's protocol. Transformed bacterial cells were plated on LB/ampicillin (50  $\mu$ g/mL) media and incubated overnight at 37 °C. Bacterial colonies were picked into LB/ampicillin broth (50  $\mu$ g/mL) and incubated overnight with shaking at 37 °C. Overnight cultures were "mini-prepped" by the boiling lysis method, extracted twice with equal volumes of phenol/chloroform and precipitated (20).

Chimeric constructs of rabbit and pig FMO1 were identified by digestion with *Nco*I. Chimeras from successful crossovers contained two *Nco*I sites, one from either rabbit FMO1 or pig FMO1 and a second from the original cloning site (Figure 1). The presence of three *Nco*I sites was indicative of a clone containing intact rabbit FMO1 and pig FMO1, presumably derived from uncut or religated pJL-rb/pig FMO1. Clones with two *Nco*I sites were sequenced by the dideoxynucleotide method (21) with sequenase (version 2.0, USB, Cleveland, OH). Tritylated oligonucleotide primers were synthesized (Applied Biosystem, model 391, Foster City), purified (ODC; Applied Biosystem, Foster City, CA), and used to identify the junctions between rabbit and pig FMO1 cDNA sequences. More precisely, the first base, reading 5' to 3', unique to the pig sequence indicated that a crossover had taken place in the area of sequence identity immediately 5' to the identified base. The first amino acid unique to the pig sequence was then identified and used to name the chimera. For example, R157P532 is a chimeric protein consisting of rabbit amino acids 1–157 and pig amino acids 158–532. It should be noted that chimeras derived from crossovers occurring 3' of codon 319 contain 535, rather than 532 residues and are designated RxxxP535. This difference is due to a nine base deletion (codons 317–319) in the pig FMO1 cDNA sequence relative to the rabbit FMO1 sequence (8).

**Construction of Complex Chimeras.** Several complex chimeras were constructed from the clones generated by the random chimeragenesis. R380P532 was digested with *Bam*HI and *Eco*RV to excise the last 78 codons and entire 3' noncoding sequence of pig FMO1. A cDNA insert, encoding residues 457–535 of rabbit FMO1, was then generated by PCR. The cDNA encoding rabbit FMO1 was used as template and primers based on the T7 promoter sequence (antisense) of pBS, and bases 1421–1440 were synthesized. The sense primer (5'ACTCCTGA CGGATC-CACTGC3') included a two base mutagenic change for introduction of a *Bam*HI site at the 5'-end of the rabbit insert. Each PCR reaction was catalyzed with 7.5 units of PFU DNA polymerase (Stratagene) at an annealing temperature of 50 °C. The insert encoding the fragment of rabbit FMO1 was purified by the Wizard PCR prep kit (Promega, Madison, WI), digested with *Bam*HI and *Eco*RV, and "in-gel" ligated to digested R379P532. *E. coli* strain XL-1 (Stratagene) was transformed with the ligated construct (R380P456R535), plated on LB/ampicillin (50  $\mu$ g/mL), and incubated overnight at 37 °C. Bacterial colonies were picked into LB/ampicillin (50  $\mu$ g/mL) broth, grown overnight with shaking at 37 °C, and "miniprep" using the alkaline lysis method. R380P456R535 chimeras were identified by digestion with *Pst*I and *Sac*I. Positive clones were sequenced as described previously.

Complex chimeras R298P358R478P532 and R157P358R478P532 were generated with the Seamless Cloning Kit (Stratagene) according to the manufacturer's

protocol. Chimeras R298P532 and R157P532, generated by random chimeragenesis, were used as templates in separate PCR reactions (Robocycler, Variable Gradient, Stratagene) to create linearized vectors from which codons 358–478 of pig FMO1 were missing. An insert consisting of rabbit FMO1 codons 361–481 was synthesized by PCR (Robocycler) from rabbit FMO1. The first 11 bases in each primer contained the *Bsm3014* restriction site, random bases, and spacer bases recommended by the manufacturer (Seamless Cloning, Stratagene). PCR amplification, restriction, ligation, and transformation of *E. coli* strain XL-1 were done according to instructions (Stratagene). The R285P532 and R157P532 cDNA clones containing inserts encoding rabbit FMO1 were identified by digestion with *StuI*. Clones identified as chimeras R285P358R478P532 and R157P358R478P532 were sequenced as described above.

**Site-Directed Mutagenesis.** Site-directed mutations were made in pJLrabbit FMO1 with a double stranded, site-directed mutagenesis kit (Chameleon, Stratagene). The selection primer (*XbaI* → *SpeI*), 5'-CCTTAGTAAGGAGAC-TA GTCCATGGCCAAGC-3', switch primer (*SpeI* → *XbaI*), 5'-CCTTAGTAAGGAGTCTA GACCATGGCCAAGC-3', and all mutagenic primers were obtained commercially (Amitof Biotech, Boston, MA). The first 21 bases of the switch and selection primers (immediately 5' of the start codon) corresponded with pJL-2 sequence. Mutagenic primers were used to convert the following amino acids present in rabbit FMO1 to those present in pig FMO1: R186S, T236M, M381L, Y391W, Q394R, F396L, I400N, K410Q, E414T, H420P, N421S, A433S, S445Y, N447D, L451M, L461H, M466I, and S472T. (These designations contain the number of the amino acid in rabbit FMO1; above number 319, the corresponding position in pig FMO1 is less by three.) Plasmids containing mutations were used to transform *E. coli* strain *mutS* as recommended (Stratagene). Subsequent cloning procedures were as described above. Clones containing the selection site were identified by digestion with *SpeI* and *KpnI* or *XbaI* and *KpnI* and sequenced as described above. Clones containing multiple mutations were constructed with the same methods described above.

**Expression and Isolation of FMO Proteins.** *E. coli* strain XL-1 was transformed (heat-shock) with cDNA encoding rabbit FMO1, rabbit FMO2, rabbit/pig FMO1 chimeras, complex chimeras, or rabbit FMO1 mutants. As noted above, the sequences of all cDNAs used for expression experiments were verified. All procedures leading to the isolation of final *E. coli* membrane fractions were as described previously (19). Pig FMO1 was purified from hepatic microsomal preparations by the method of Sabourin et al. (22).

**Analysis of Catalytic Activities.** The ability of the expressed and purified forms of FMO1 to metabolize methimazole was assessed by the spectrophotometric (Aminco DW2A, UV-Vis spectrophotometer) method of Dixit and Roche (23). Determination of methimazole activity as a measure of enzyme content has been demonstrated by comparison with immunochemical quantitation and flavin content (24). The effects of imipramine on methimazole metabolism were determined by addition of aqueous imipramine to the sample and reference cuvettes after obtaining a stable rate of methimazole oxidation (13). Metabolism of

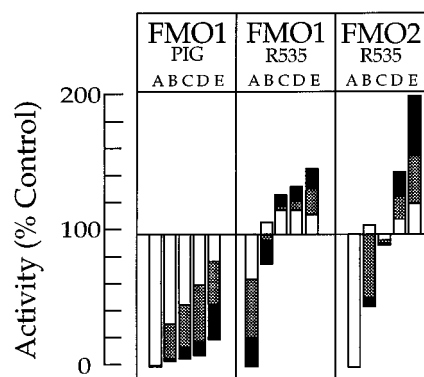


FIGURE 2: Modulation by imipramine of the metabolism of methimazole catalyzed by purified pig FMO1 and recombinant rabbit FMO1 and FMO2. The rate of metabolism was determined at five concentrations of methimazole (A, 1  $\mu$ M; B, 50  $\mu$ M; C, 100  $\mu$ M; D, 300  $\mu$ M; and E, 1 mM) and three concentrations of imipramine (solid portion, 750  $\mu$ M; spotted portion, 300  $\mu$ M; and white portion, 50  $\mu$ M). The activities are shown as percent control (activity in the absence of imipramine).

imipramine was determined by following substrate-dependent oxidation of NADPH at 340 nm. The assay contained tricine/KOH (0.1 M, pH 8.4), EDTA (1 mM), NADPH (0.1 mM), and sample protein in total volume of 1 mL.

## RESULTS

**The Effect of Imipramine on the Metabolism of Methimazole Catalyzed by Pig and Rabbit FMO1 and Rabbit FMO2.** Our initial results demonstrate that imipramine can be an inhibitor or an activator of the same FMO isoform. Which of the two is observed depends on two factors, the concentration of methimazole and the specific FMO isoform (Figure 2). In either case, inhibition or activation, a direct relationship between the magnitude of the effect and the concentration of imipramine is observed. With the rabbit homologues, FMO1 and FMO2, activation is observed at higher concentrations of methimazole and inhibition at lower concentrations. The methimazole concentration at which no effect is observed (activation = inhibition) at any concentration of imipramine is  $\sim$ 100  $\mu$ M with FMO2 and  $\sim$ 50  $\mu$ M with FMO1. Activation of FMO2 exceeds that of FMO1 (2-fold vs 1.5-fold at a methimazole concentration of 1 mM) and FMO2 is more sensitive than FMO1 to inhibition by imipramine at low concentrations ( $<$ 100  $\mu$ M) of methimazole (Figure 2).

In contrast to results obtained with rabbit FMO1 and FMO2, imipramine inhibits the activity of pig FMO1 at all concentrations (1 mM to 1 mM) of methimazole examined (Figure 2). The inhibition appears competitive with an  $I_{50}$  that is less than the  $K_m$  for methimazole; reactions containing equimolar concentrations of imipramine and methimazole are inhibited by greater than 50%. It should be noted that the same  $K_m$  ( $\sim$ 3  $\mu$ M) for methimazole is obtained with both pig FMO1 and rabbit FMO1 (refer to Figure 4), whereas the  $K_m$  with FMO2 is about 300  $\mu$ M (13). Inhibition of FMO2 by imipramine also appears to be competitive, although it occurs only when the imipramine concentration is much greater than the methimazole concentration. This finding is consistent with detection of imipramine-dependent, FMO2-catalyzed oxidation of NADPH that is less than 10% of that observed with methimazole (not shown).

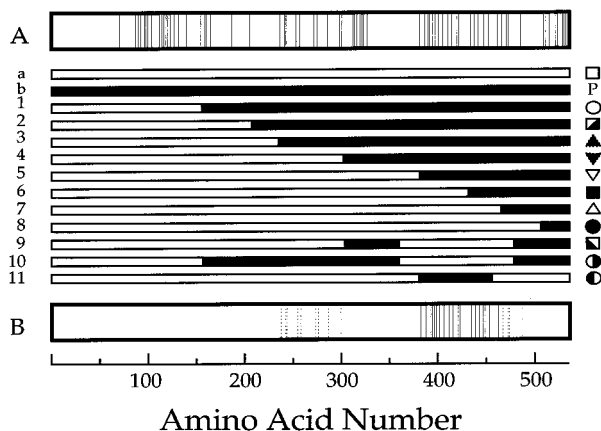


FIGURE 3: Diagram of chimeras formed between rabbit and pig orthologs of FMO1. The chimeras formed by random chimeragenesis (1–8) between rabbit FMO1 (a, □) and pig FMO1 (b, P) are referred to by the following names and symbols as shown: 1, R157P532, ○; 2, R205P532, ▣; 3, R235P532, ▲; 4, R298P532, ▼; 5, R380P535, ▽; 6, R432P535, ■; 7, R465P535, △; 8, R507P535, I. In addition, several complex chimeras (9–11) were examined: 9, R298P358R478P532, ▣; 10, R157P358R478P532, ●; 11, R380P456R535, ○. The symbols are used in Figures 4–9. Positions of amino acid differences between pig and rabbit FMO1 are shown in panel A and position differences remaining to be considered following analysis of the chimeras are shown in panel B (solid lines indicate strongly positive possibilities and dashed lines indicate weakly positive possibilities). The nomenclature used for the chimeras is explained in the *Materials and Methods*.

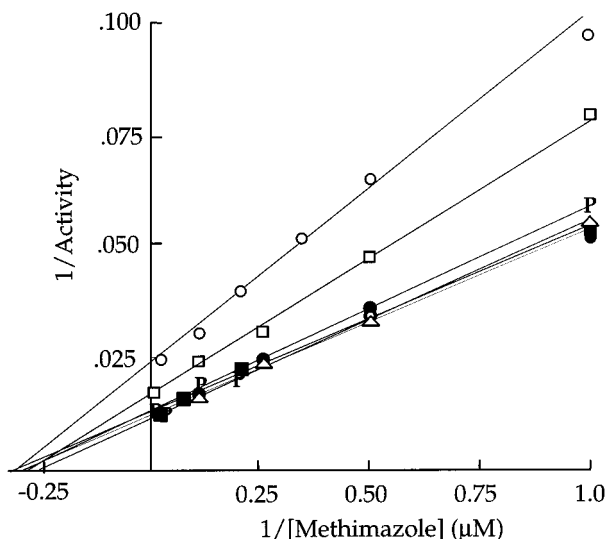


FIGURE 4: Lineweaver–Burke plot for the metabolism of methimazole catalyzed by pig and rabbit FMO1 and selected chimeras. Results are shown for rabbit FMO1 (□), pig FMO1 (P), and the chimeras R465P535 (△), R507P535 (I) and R432PP535 (■), R157P532 (○). Activity is expressed as nanomole of product  $\times$  milligrams of protein $^{-1} \times$  min $^{-1}$ .

Our results are unique for the FMO in that they differentiate between orthologs (pig and rabbit FMO1) that are 87% identical much more clearly than between homologues (rabbit FMO1 and FMO2) that are only 56% identical. The high identity between rabbit and pig FMO1 allowed us to take advantage of random chimeragenesis (15, 16) for investigation of structural differences between the FMO1 orthologs related to their observed functional variance.

**Production and Characterization of Pig FMO1/Rabbit FMO1 Chimeras.** From 3 to 10 unique chimeras were recovered from a single transformation of *E. coli* strain

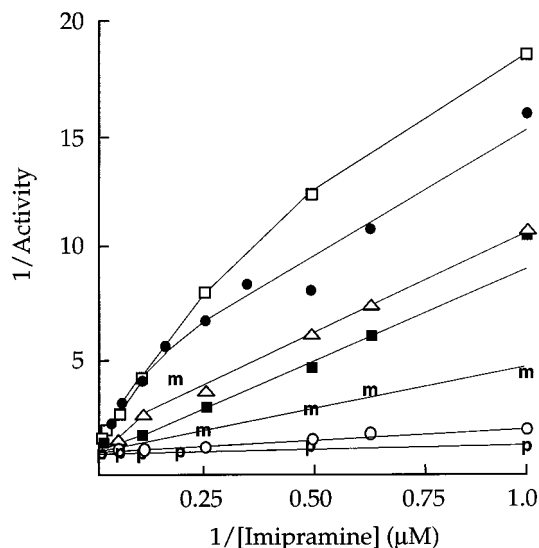


FIGURE 5: Lineweaver–Burke plot for imipramine-dependent NADPH oxidation catalyzed by rabbit and pig FMO1 and selected chimeras. Results are shown for rabbit FMO1 (□), pig FMO1 (P), and the chimeras R507P535 (I), R465PP535 (△), R432P535 (■), and R157P532 (○). The results for mutant 10 (m) are also shown (see Figure 10). The activities reported are nanomole of NADPH oxidized  $\times$  minute $^{-1} \times$  (nanomole of methimazole metabolized  $\times$  minute $^{-1} \times$  milligrams of protein $^{-1}$ ) $^{-1}$ .

NM522 or JM101 with linearized pJL-rabbit/pig FMO1 plasmid (1  $\mu$ g). Of the 32 different chimeras that yielded metabolically active proteins when expressed in *E. coli*, eight were characterized in detail. All chimeras produced by random chimeragenesis contained a minimum of the first 130 codons of the rabbit sequence owing to the location of the *Dra*III restriction site used for linearization. The decision to utilize the *Dra*III site was prompted by two factors. First, we have been unable to express full-length pig FMO1 or rabbit(5′)/pig(3′)-FMO1 restriction fragment chimeras containing less than  $\sim$ 300 nucleotides of rabbit sequence at levels that allow for characterization (M. Lawton, unpublished observations). Second, we have reported that regulation of the imipramine interaction with FMO1 is a function of the C-terminal half of the enzyme (25).

The chimeras formed by random chimeragenesis and characterized were R157P532, R205P532, R235P532, R298P532, R380P535, R432P535, R465P535, and R507P535. In addition, complex chimeras (see Materials and Methods) R380P456R535, R298P358R478P532, and R157P358R478P532 were examined. The spatial relationships between the chimeric junctions and differences between the sequences of rabbit and pig FMO1 are shown in Figure 3.

**Metabolism of Methimazole and Imipramine.** The metabolism of methimazole catalyzed by pig FMO1, rabbit FMO1, and rabbit/pig chimeras is shown in Figure 4. The data, expressed in the form of a Lineweaver–Burke plot, show the same  $K_m$  for methimazole ( $\sim$ 3  $\mu$ M) for all forms of the enzyme. Differences in activities (20–70 nmol of product  $\times$  mg protein $^{-1} \times$  min $^{-1}$ ) reflect variable levels of expression with different forms of the enzyme and different preparations of the same form. In contrast to the results with methimazole, the kinetics of the metabolism of imipramine with different forms of the enzyme were highly variable (Figure 5). Data with pig FMO1 are linear with a  $K_m$  of

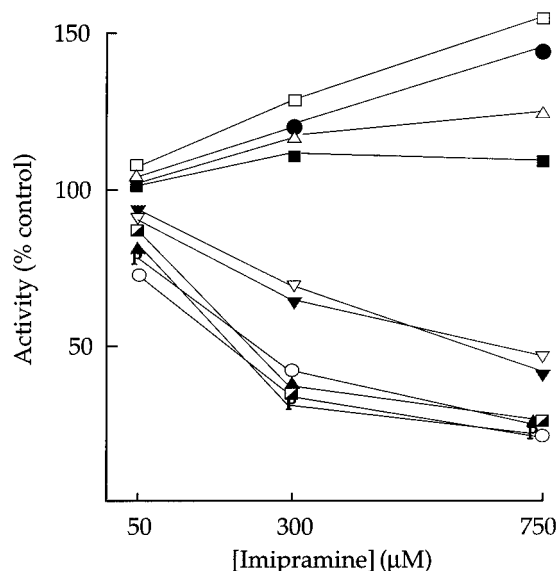


FIGURE 6: Effect of imipramine on the metabolism of methimazole (1 mM) catalyzed by rabbit and pig FMO1 and selected chimeras. The effects of three concentrations (50, 300, and 750  $\mu\text{M}$ ) of imipramine on the metabolism of methimazole (1 mM) are shown as a percent of control activity (no imipramine). Rates of metabolism catalyzed by rabbit ( $\square$ ) and pig (P) FMO1 and chimeras R507P535 ( $\square$ ), R465PP535 ( $\Delta$ ), R432P535 ( $\blacksquare$ ), R380P535 ( $\nabla$ ), R298P532 ( $\blacktriangledown$ ), R235P532 ( $\blacktriangle$ ), R205P532 ( $\blacksquare$ ), and R157P532 ( $\circ$ ) are shown.

$\sim 0.5 \mu\text{M}$  (estimated from a range of concentrations lower than those shown), whereas the data with rabbit FMO1 are markedly curvilinear with disproportional increases in activity with increasing substrate concentration. The extent of the curvilinearity is inversely related to the amount of pig FMO1 included at the carboxy end of the chimeric proteins. Linear results, similar to those with pig FMO1, are obtained with R157P532. With imipramine as the substrate, the variability observed reflects differences in enzyme properties as the imipramine activity is reported per unit methimazole activity. In all cases, however, maximum rates of metabolism, estimated by visual extrapolation of the curves shown in Figure 5, appear to be similar,  $\sim 1 \text{ nmol} \times \text{min}^{-1} \times \text{nmol}$  of methimazole metabolized $^{-1}$ .

#### Modulation of Methimazole Metabolism by Imipramine.

The effects of imipramine (50, 300, and 750  $\mu\text{M}$ ) on metabolism of methimazole (1 mM) catalyzed by various forms of FMO1 are shown in Figure 6. Under these conditions, rabbit FMO1 is activated and pig FMO1 is inhibited, both in a concentration-dependent manner (see Figure 2). The responses of the chimeras relative to the two wild-type enzymes can be described in one of four ways: first, little alteration of the rabbit FMO1 response (R507P535); two, marked reduction in activation, but no inhibition (R465P535 and R432P535); third, elimination of activation and introduction of significant inhibition (R380P535 and R298P532); fourth, inhibition characteristic of pig FMO1 (R235P532, R205P532, and R157P532). Similar results were obtained for metabolism of methimazole at 100  $\mu\text{M}$  (Figure 7) except that the change in response with R432P535 was now clearly greater than observed with R465P535. The results at 100  $\mu\text{M}$ , like those at 1 mM, showed no differences between R380P535 and R298P532 or among R235P532, R205P532, R157P532, and pig FMO1. The similarity of R235P532, R205P532, R157P532, and pig FMO1 was also evident at a methimazole concentration of 1  $\mu\text{M}$  (Figure 8).

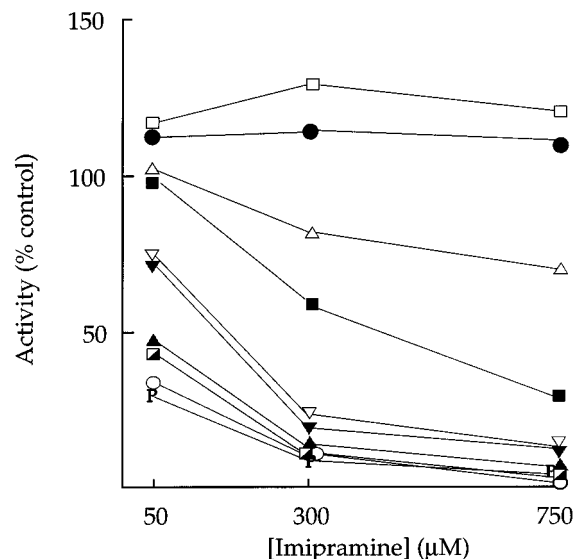


FIGURE 7: Effect of imipramine on the metabolism of methimazole (100  $\mu\text{M}$ ) catalyzed by rabbit and pig FMO1 and selected chimeras. The effects of three concentrations (50, 300, and 750  $\mu\text{M}$ ) of imipramine on the metabolism of methimazole (100  $\mu\text{M}$ ) are shown as a percent of control activity (no imipramine). Rates of metabolism catalyzed by rabbit ( $\square$ ) and pig (P) FMO1 and chimeras R507P535 ( $\square$ ), R465PP535 ( $\Delta$ ), R432P535 ( $\blacksquare$ ), R380P535 ( $\nabla$ ), R298P532 ( $\blacktriangledown$ ), R235P532 ( $\blacktriangle$ ), R205P532 ( $\blacksquare$ ), and R157P532 ( $\circ$ ) are shown.

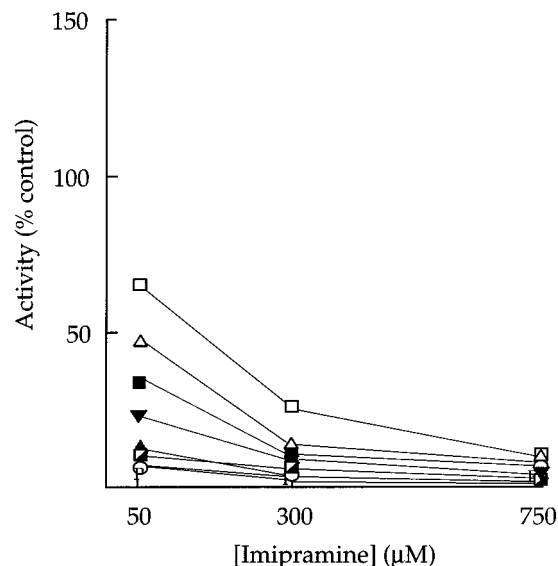


FIGURE 8: Effect of imipramine on the metabolism of methimazole (1  $\mu\text{M}$ ) catalyzed by rabbit and pig FMO1 and selected chimeras. The effects of three concentrations (50, 300, and 750  $\mu\text{M}$ ) of imipramine on the metabolism of methimazole (1 mM) are shown as a percent of control activity (no imipramine). Rates of metabolism catalyzed by rabbit ( $\square$ ) and pig (P) FMO1 and chimeras R507P535 ( $\square$ ), R465PP535 ( $\Delta$ ), R432P535 ( $\blacksquare$ ), R298P532 ( $\blacktriangledown$ ), R235P532 ( $\blacktriangle$ ), R205P532 ( $\blacksquare$ ), and R157P532 ( $\circ$ ) are shown.

The results with R157P532 and pig FMO1 at all concentrations of methimazole confirmed our earlier conclusion that variations in the N-terminal portion of the protein do not contribute to the difference between the responses of rabbit FMO1 and pig FMO1 to imipramine (25) and validated use of the *Dra*III site in the random chimeragenesis procedure.

Amino acids 381–432 and 433–465 were identified from the properties of the simple chimeras as regions of FMO1 with major influence on the imipramine interaction. Minor effects could be attributed to regions 236–298 and 466–

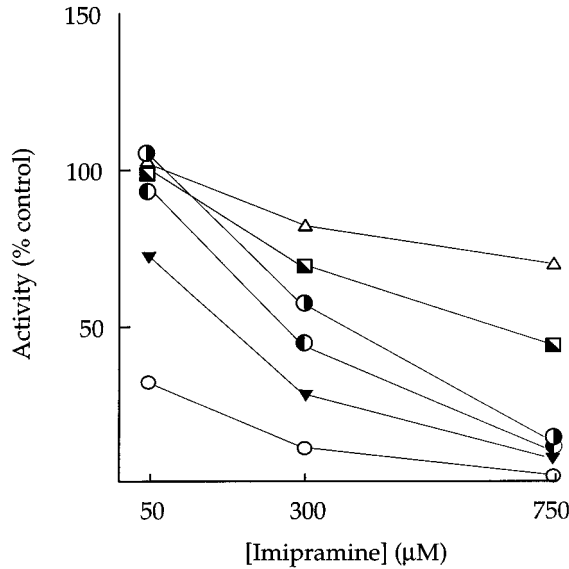


FIGURE 9: Effect of imipramine on the metabolism of methimazole (100  $\mu$ M) catalyzed by complex and parent chimeras. The effects of three concentrations (50, 300, and 750  $\mu$ M) of imipramine on the metabolism of methimazole (100 mM) are shown as a percent of control activity (no imipramine). Rates of metabolism catalyzed by complex chimeras R298P358R478P532 (■), R157P358R478P532 (●), and R380P456R535 (●) and parent chimeras R465PP535 (Δ), R298P532 (▼), and R157P532 (○) are shown.

507, whereas regions 1–235, 299–380, and 508–535 appeared to have no influence on the imipramine effect. Of the 70 amino acid differences between pig and rabbit FMO1, 12 are in the 381–432 region, seven in the 433–465 region, and a total of 12 in the 236–298 and 466–507 regions. Results obtained with complex chimeras confirmed the importance of the area from 381 to 465 in the imipramine interaction (Figure 9). First, insertion of rabbit sequence 359–478 into the chimera R157P532 to form R157P358R478P532 or into R298P532 to form R298P358R478P532 eliminated inhibition of methimazole (100  $\mu$ M) metabolism by imipramine (50  $\mu$ M) and significantly decreased inhibition by higher concentrations of imipramine (300 and 750  $\mu$ M). Second, replacement of rabbit sequence 381–456 with the corresponding sequence from pig to form R380P456R535 eliminated the slight activation observed at all concentrations of imipramine with rabbit FMO1 and resulted in 50 and 80% inhibition at 300 and 750  $\mu$ M imipramine, respectively.

**Identification of Specific Amino Acids Involved in the Imipramine Interaction.** Critical amino acids were identified by changing residues in rabbit FMO1 to the corresponding residues found in pig FMO1. A total of 20 mutants containing 1–9 amino acid changes were characterized (Table 1). The following substitutions, made singly or in conjunction with other changes, had no effect on the 1.25-fold activation of methimazole (100  $\mu$ M) metabolism by imipramine (750  $\mu$ M) observed with rabbit FMO1: Y391W, F396L, K410Q, E414T, N447D, and L452M (Figure 10, mutants 1–5). Several of these mutations (F396L, K410Q, E414T, and L452M) were also negative in combination with mutations shown to be effective (Figure 10, mutants 10–12). In addition, E386D, Q394R, and S445Y did not alter the properties of moderately effective mutants (Figure 10, mutants 10, 11, and 13), and T236M, L461H, M466I, and S472T did not increase the extent of inhibition observed with

Table 1: Mutants of Rabbit FMO1 Containing Amino Acids Present in Pig FMO1

1	N447D						
2	K410Q						
3	K410Q	E414T					
4	F396L	L452M					
5	Y391W						
6	I400N						
7	H420P						
8	M381L						
9	M381L	I400N					
10	M381L	E386D	Q394R	F396L	I400N	K410Q	E414T
11	M381L	Q394R	F386L	I400N	K410Q	E414T	L452M
12	R186S	L452M					
13	R186S	M381L	I400N	S445Y			
14	R186S	M381L	I400N				
15	M381L	F396L	I400N	A433S			
16	R186S	M381L	LF396L	I400N	A433S		
17	R186S	M381L	F396L	I400N	H420P	A433S	
18	R186S	M381L	F396L	I400N	H420P	A433S	L461H S472T
19	R186S	T236M	M381L	F396L	I400N	H420P	A433S L461H S472T
20	R186S	M381L	F396L	I400N	H420P	A433S	L461H M466I S472T

<sup>a</sup> The entries include the amino acid present in rabbit FMO1 followed by the amino acid number in the rabbit sequence and the residue present in pig FMO1.

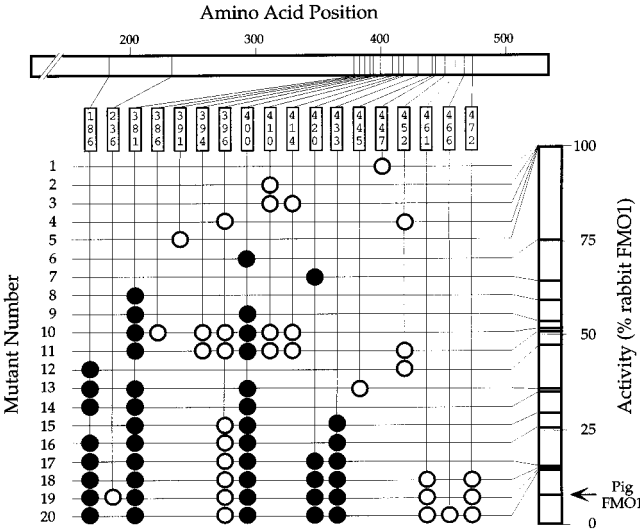


FIGURE 10: Effects of imipramine (750  $\mu$ M) on the metabolism of methimazole (100  $\mu$ M) catalyzed by mutants of rabbit FMO1. Single (1, 2, 5–8) and multiple (3, 4, 9–20) mutants of rabbit FMO1 were expressed in *E. coli* and examined for the effect of imipramine (750 mM) on the metabolism of methimazole (100  $\mu$ M). All mutations were to amino acids present in pig FMO1. Mutations that produce a change in response are designated by the closed circles (●) and those that were without effect are designated by open circles (○). The activities of the mutants as a percent of the wild type (rabbit FMO1) are shown (100% = 1.3-fold activation) on the right-hand side of the figure and the mutant numbers are shown on the left-hand side. The amino acid numbers and relative positions in the protein are shown at the top of the figure. Amino acid changes are listed in Table 1.

highly effective combinations (Figure 10, mutants 18–20). In contrast, several single changes (I400N, H420P, and M381L) resulted in mutants whose activities were only 72, 63, and 59%, respectively, of the activity with rabbit FMO1 (Figure 10, mutants 6–8).

Results with mutants containing multiple changes indicated the importance of two additional positions, 186 and 433. The activity of mutant 12 containing R186S and L452M (negative) was only 46% of rabbit FMO1 (Figure 10), and the addition of A433S and F396L (negative) to a mutant containing M381L and I400N decreased activity from 54 to 29% of the control (Figure 10, mutants 9 and 15). Combina-

tion mutants showed that the effects of M381L, I400N, and A433S were at least partially independent (Figure 10, mutants 9 and 15). This was also the case for R186S when added to M381L and I400N (decrease from 54 to 36% of control activity; mutants 9 and 14). However, addition of R186S to M381L, I400N, and A433S had little or no effect (mutants 15 and 16). In contrast, addition of H420P to R186S, M381L, I400N, and A433S (mutants 16 and 17) decreased activity from 25 to 15% of control. The effect of imipramine on metabolism of methimazole with combination mutants (17–20) containing R186S, M381L, I400N, H420P, and A433S (~15% of control activity) approached that observed with chimera R157P532 or pig FMO1 (~7.5% of control activity). In addition, the kinetics of methimazole metabolism catalyzed by these mutants were the same as for the wild-type rabbit and pig FMO1 orthologs (see Figure 2), whereas the kinetics for imipramine metabolism most closely resembled those of pig FMO1 (see Figure 3).

## DISCUSSION

It has been known for some time that activation of FMO-catalyzed reactions is dependent upon the activator molecule and the FMO isoform. The activity of FMO1 purified from pig liver is increased by the addition of alkylguanidines and primary, secondary and short-chain tertiary alkylamines (10, 26, 27). The model activator for pig FMO1, *n*-octylamine, also activates rabbit FMO1 but has no effect on FMO2 (13, 14). In contrast, imipramine and other tricyclic antidepressants have been reported to be activators of FMO2 but not of rabbit FMO1 (13). These differential effects appear to be related to the status of the activator as a substrate; *n*-octylamine is a substrate for FMO2 but not for FMO1 (11, 12), and imipramine is a substrate for FMO1 (22, 28) but has been reported not to be a substrate for FMO2 (14).

Initial results of the present study show that the interactions of imipramine with rabbit FMO1 and FMO2 are more complicated than recognized previously (13). Although imipramine does activate FMO2, activation is confined to substrate concentrations > 100  $\mu$ M. At lower concentrations of methimazole (<100  $\mu$ M), imipramine acts as an inhibitor of FMO2. Similar results are obtained for rabbit FMO1 with no apparent modulation (activation = inhibition) observed at a methimazole concentration of ~50  $\mu$ M. The reported lack of effect of imipramine on rabbit FMO1 (13) is explained by the substrate concentration used in that study which was 30  $\mu$ M (10  $k_m$ ). The magnitude of the imipramine effect on the activity of rabbit FMO1 or FMO2 is a function of both the substrate and the modulator (activator/inhibitor) concentrations.

In contrast to its effects on rabbit FMO1 and FMO2, imipramine is an inhibitor of pig FMO1 at all substrate concentrations tested. Thus, the activation site of pig FMO1, hypothesized on the basis of results with a number of compounds (10, 26, 27), excludes imipramine. The difference between the responses of pig and rabbit FMO1 provides a good starting point for investigating the nature of the interaction of modulators with the FMO. A study of the rabbit and pig orthologs was also prompted by their high sequence identity (87%), which made the application of random chimeragenesis feasible (15, 16).

Results with simple chimeras produced by random chimeragenesis indicate that the balance between activation and

inhibition of FMO activity is controlled by discrete regions of the FMO molecule, a conclusion reinforced by findings with complex chimeras.

A stepwise transition from the properties of rabbit FMO1 to those of pig FMO1 was evident in a series of chimeras containing increasing amounts of the pig enzyme. This transition entailed simultaneous changes in several parameters: first, the response at high substrate concentrations changed progressively from activation to inhibition; second, inhibition at low substrate concentrations increases progressively; third, self-activation of imipramine metabolism diminished progressively. These characteristics were altered without any change in the  $K_m$  for methimazole. The values obtained ranged from 2.5 to 3.3  $\mu$ M for all forms (wild-type, chimeras, and mutants) of the enzyme examined and are consistent with values of 3.8  $\mu$ M and 5  $\mu$ M reported previously for rabbit FMO1 (13) and pig FMO1 (26), respectively.

With the purified pig enzyme and pig-like chimeras, the metabolism of imipramine follows Michaelis–Menton kinetics with no evidence of self-activation and a  $V_{max}$  similar to that for methimazole. The kinetics of the metabolism of imipramine by rabbit FMO1, which show evidence for self-activation, are similar to those observed by Ziegler et al. (10) for the metabolism of *N,N*-dimethyloctylamine by pig FMO1. Other proposed examples of substrate activation of FMO activity (29, 30) appear to be confounded by the participation of multiple FMO isoforms in the reactions (13).

Inhibition of pig FMO1 by imipramine at all substrate concentrations is consistent with both the absence of self-activation and a  $K_m$  value that is significantly less than that for methimazole (~0.5 vs 3  $\mu$ M). Imipramine is also a substrate for rabbit FMO1, but with a much lower apparent affinity than for the pig ortholog. The relationship between the ability of imipramine to act as an inhibitor and its behavior as a substrate is reinforced by our findings with FMO2. Inhibition of FMO2 activity is observed at substrate concentrations < 100  $\mu$ M and with imipramine concentrations in excess of the substrate concentration. These results can be explained by low, but detectable imipramine metabolism even with a  $K_m$  likely higher than the highest substrate concentration (1 mM) that could be examined. Inhibition occurs because the  $K_m$  for methimazole (300  $\mu$ M) with FMO2 is also quite high (13), 2 orders of magnitude greater than with FMO1. In cases where no modulator metabolism can be detected, as in the interaction of *n*-octylamine with pig FMO1, activation is seen at all substrate concentrations (10).

Results with chimeras were used as a guide for altering rabbit FMO1 by site-directed mutagenesis. The difference between the responses of rabbit and pig FMO1 to imipramine was found to be regulated by as few as five amino acids. Changes at positions 381 (leucine for methionine), 400 (asparagine for isoleucine), and 433 (serine for alanine) elicit effects that are at least partially additive. Of these changes, only the one at 400 involves an obvious difference according to the classification of Bardo et al. (31), although the change at 381 could be related to a decrease in side-chain flexibility (32). The effect of the change at position 420 (proline for histidine), which is profound when introduced alone, is somewhat negated in the presence of changes at 186, 381, 400, and 433. Of some interest is the substitution of serine

for arginine at position 186. Because of its proximity to the NADPH binding domain, this position is a good candidate for involvement with activation, which results from an increase in  $V_{\max}$  (26). With the FMO,  $V_{\max}$  is not related to the substrate and is thought to involve the rate of hydrolysis of the flavin pseudobase (33, 34). A change at 186, in the absence of any changes at the other critical positions, produces the largest single effect observed. This change is also effective when made in combination with changes at 381 and 400, but not when 433 is also added to the list. Similar results are seen with the chimeras. First, R157P532 and R205P532 (presence or absence of R186S in the presence of A433S) have the same properties; second, chimera R157P358R478P532 is much more like pig FMO1 than chimera R298P358R478P532 (presence or absence of R186S in the absence of A433S). The effects of amino acids other than those present in pig or rabbit FMO1 on the interaction between positions 186 and 433 are now being investigated.

Our results confirm the conclusions of Ziegler and co-workers (10, 26, 27) that the FMO contains a regulatory site that is distinct from the catalytic site. In addition, we propose that imipramine can occupy two distinct positions within the regulatory site, one that results in activation by increasing the  $V_{\max}$  and one that results in inhibition through some competitive mechanism directly associated with its metabolism. As the interaction of imipramine with the FMO, both as a substrate and as a modulator, are altered simultaneously without modification of the kinetic parameters associated with the metabolism of methimazole, we conclude that the site of inhibition must be distinct from the catalytic site. This suggests competition for activated oxygen rather than for a binding site as the mechanism of inhibition.

Although it is clear that the responses of pig and rabbit FMO1 to imipramine depend on the amino acids present at a limited number of positions, the relationships between these residues and overall structure are unknown. The absence of a crystalline structure for the mammalian FMO makes modeling the imipramine interaction difficult, but recent results with trypanothione reductase (TR) may provide a starting place. TR, which contains similar FAD and NADPH binding domains to those present in FMO1 (35, 36), interacts with a number of compounds, including imipramine, that are known to modulate FMO activity (36, 37). A number of these compounds are inhibitors of TR but do not interact with glutathione reductase (GR), the structure of which closely resembles that of TR (36). It is noteworthy that the 3-dimensional structures of TR and GR have been resolved and that the specificity of the interaction with these compounds is understood at the molecular level (36, 38, 39). These findings may be of value in attempts to construct a model of the FMO.

Our results represent the first step in deciphering the structural parameters that determine how FMO activity is modulated by amine compounds, as first described by Ziegler et al. (10). The final solution will need to account for a number of diverse outcomes that range from activation only to inhibition only and are dependent upon FMO isoform, modulator compound, and substrate concentration.

## REFERENCES

1. Ziegler, D. M. (1993) *Annu. Rev. Pharmacol. Toxicol.* 33, 179–99.
2. Lawton, M. P., Philpot, R. M. in *Reviews in Biochemical Toxicology* Hodgson, E., Bend, J. R., and Philpot, R. M. Eds.) Vol. 11, pp 1–27, Toxicological Communications, Inc., Raleigh, NC.
3. Lawton, M. P., Cashman, J. R., Cresteil, T., Dolphin, C. T., Elfarra, A. A., Hines, R. N., Hodgson, E., Kimura, T., Ozols, J., Phillips, I. R., Philpot, R. M., L Poulsen, L., Rettie, A. E., Shepard, E. A., Williams, D. E., and Ziegler, D. M. (1994) *Arch. Biochem. Biophys.* 308, 254–257.
4. Devereux, T. R., Philpot, R. M., and Fouts, J. R. (1977) *Chem.-Biol. Interact.* 18, 277–287.
5. Tynes, R. E., Sabourin, P. J., and Hodgson, E. (1985) *Biochem. Biophys. Res. Commun.* 126, 1069–1075.
6. Williams, D. E., Ziegler, D. M., Nordin, D. J., Hale, S. E., and Masters, B. S. S. (1984) *Biochem. Biophys. Res. Commun.* 125, 116–122.
7. Gasser, R., Tynes, R. E., Lawton, M. P., Korsemyer, K. K., Ziegler, D. M., Philpot, R. M. (1990) *Biochemistry* 29, 119–124.
8. Lawton, M. P., Gasser, R., Tynes, R. E., Hodgson, E. and Philpot, R. M. (1990) *J. Biol. Chem.* 265, 5855–5861.
9. Hines, R. N., Cashman, J. R., Philpot, R. M., Williams, D. E., and Ziegler, D. M. (1994) *Toxicol. Appl. Pharmacol.* 125, 1–6.
10. Ziegler, D. M., Poulsen, L. L., and McKee, E. M. (1971) *Xenobiotica* 1, 523–531.
11. Tynes, R. E., Sabourin, P. J., Hodgson, E., and Philpot, R. M. (1986) *Arch. Biochem. Biophys.* 251, 654–664.
12. Poulsen, L. L.; Taylor, K., Williams, D. E., Masters, B. S. S., and Ziegler, D. M. (1986) *Mol. Pharmacol.* 30, 680–685.
13. Lawton, M. P., Kronbach, T., Johnson, E. F., and Philpot, R. M. (1991) *Mol. Pharm.* 40, 692–698.
14. Williams, D. E., Hale, S. E., Muerhoff, A. S., and Masters, B. S. S. (1985) *Mol. Pharm.* 28, 381–390.
15. Chen, M.-Y., Devreotes, P. N., and Gundersen, R. E. (1994) *J. Biol. Chem.* 269, 20925–20930.
16. Kim, J.-Y., and Devreotes, P. N. *J. Biol. Chem.* (1994) 269, 28724–28731.
17. Pernecky, S. J., Larson, J. R., Philpot, R. M., and Coon, M. J. (1993) *Proc. Natl. Acad. Sci.* 90, 2651–2655.
18. Burnett, V. B., Lawton, M. P., and Philpot, R. M. (1994) *J. Biol. Chem.* 269, 14314–14322.
19. Lawton, M. P., and Philpot, R. M. (1993) *J. Biol. Chem.* 268, 5728–5734.
20. Sambrook, J., Fritsch, E. F., and Maniatis, T. (1989) *Molecular Cloning: A laboratory manual*, 2nd ed.; Cold Spring Harbor Laboratory Press, Plainview, NY.
21. Sanger, F., Nicklen, S., and Coulson, A. R. (1977) *Proc. Natl. Acad. Sci. U.S.A.* 74, 5463–5467.
22. Sabourin, P. J., and Hodgson, E. (1984) *Chem.-Biol. Interact.* 51, 125–139.
23. Dixit, A., and Roche, T. E. (1984) *Arch. Biochem. Biophys.* 223, 50–63.
24. Overby, L. H., Buckpitt, A., Lawton, M. P., Atta-Asafo-Adjei, E., Schulze, J., and Philpot, R. M. (1995) *Arch. Biochem. Biophys.* 317, 275–284.
25. Philpot, R. M., Atta-Asafo-Adjei, E., Nikbakht, K., Burnett, V., and Lawton, M. P. (1994) in *Molecular Aspects of Oxidative Drug Metabolizing Enzymes: Their Significance in Environmental Toxicology, Chemical Carcinogenesis and Health* (Arinc, E., Hodgson, E., and Schenkman, J., Eds.) NATO ASI Series, Springer-Verlag, London.
26. Poulsen, L. L. (1991) in *Chemistry and Biochemistry of Flavoproteins* (Miller, F., Ed.) Vol. 2, pp 87–100, CRC Press, Boca Raton, FL.
27. Ziegler, D. M. (1980) in *Enzymatic Basis of Detoxication* (Jakoby, W. B., Ed) Vol. 1 pp 201–227, Academic Press, New York.
28. Cashman, J. R., and Ziegler, D. M. (1986) *Mol. Pharmacol.* 29, 163–167.



29. Cashman, J. R., and Hanzlik, R. P. (1981) *Biochem. Biophys. Res. Commun.* 98, 147–153.
30. Tynes, R. E., and Hodgson, E. (1985) *Arch. Biochem. Biophys.* 240, 77–93.
31. Bardo, D., and Argos, P. (1991) *J. Mol. Biol.* 217, 721–729.
32. Richardson, J. S., and Richardson, D. C. (1989) in *Predication of Protein Structure and the Principles of Protein Confirmation* (Fasman, G., Ed.) pp 1–88, Plenum Publishing, New York.
33. Beaty, N. B., and Ballou, D. P. (1981) *J. Biol. Chem.* 256, 4611–4618.
34. Beaty, N. B., and Ballou, D. P. (1981) *J. Biol. Chem.* 256, 4619–4625.
35. Atta-Asafo-Adjei, E., Lawton, M. P., and Philpot, R. M. (1993) *J. Biol. Chem.* 268, 9681–9689.
36. Krauth-Siegel, R. L., and Schöneck, R. (1995) *FASEB J.* 9, 1138–1146.
37. Benson, T. J., McKie, J. H., Garforth, J., Borges, A., Fairlamb, A. H., and Douglas, K. T. (1992) *Biochem. J.* 286, 9–11.
38. Karplus, P. A., Pai, E. F., and Schulz, G. E. (1989) *Eur. J. Biochem.* 178, 693–703.
39. Sullivan, F. X., Sobolov, S. B., Bradley, M., and Walsh, C. T. (1991) *Biochemistry* 30, 2761–2767.

BI972622B